doi.org/10.1002/cplu.202000248

Imaging of Monoamine Neurotransmitters with Fluorescent Nanoscale Sensors

Meshkat Dinarvand,[a] Sofia Elizarova,[b] James Daniel,[b] and Sebastian Kruss*[a]

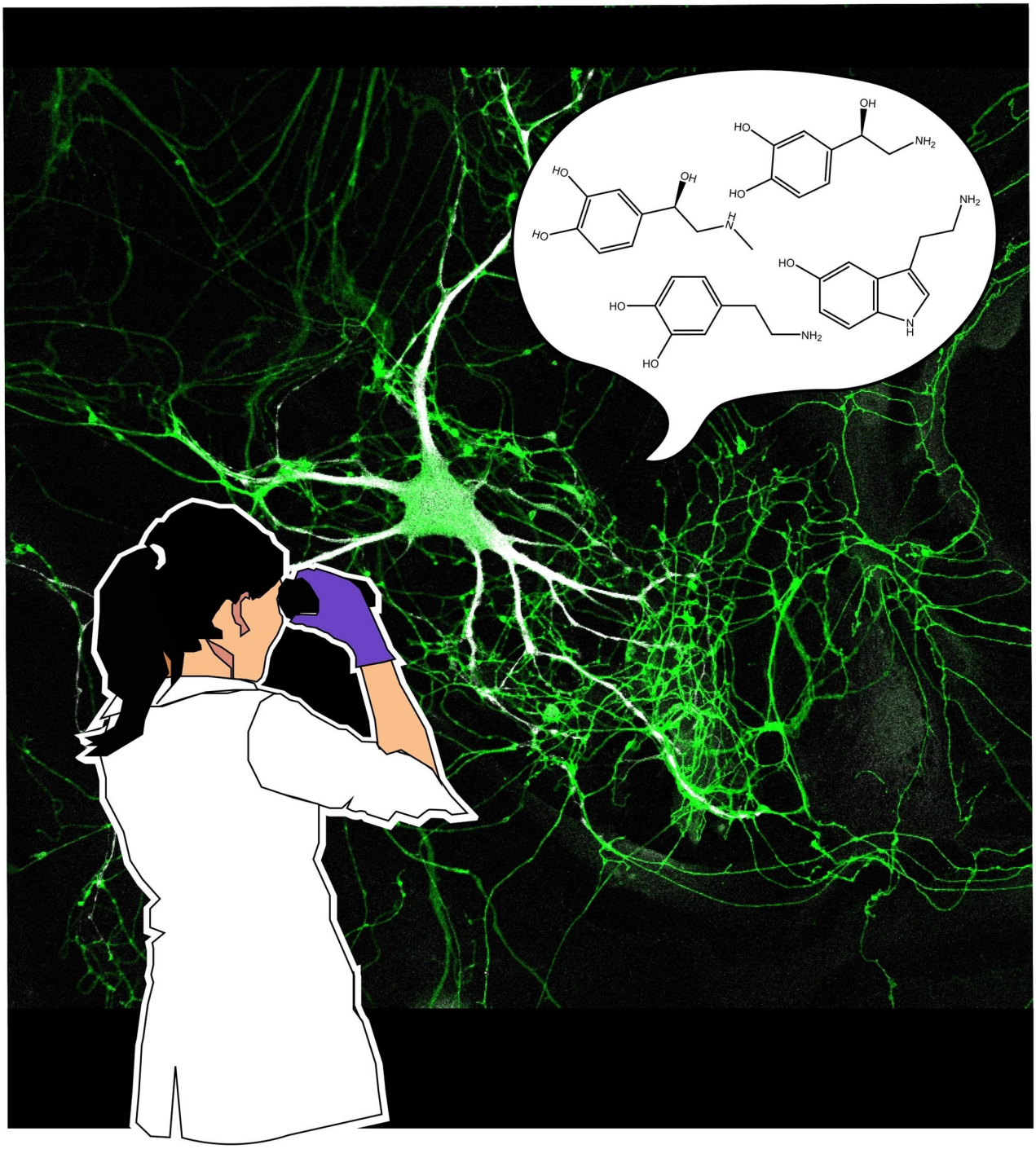

Cells use biomolecules to convey information. For instance, neurons communicate by releasing chemicals called neurotransmitters, including several monoamines. The information transmitted by neurons is, in part, coded in the type and amount of neurotransmitter released, the spatial distribution of release sites, the frequency of release events, and the diffusion range of the neurotransmitter. Therefore, quantitative information about neurotransmitters at the (sub)cellular level with high spatiotemporal resolution is needed to understand how complex cellular networks function. So far, various analytical methods have been developed and used to detect neurotransmitter secretion from cells. However, each method has limitations with respect to chemical, temporal and spatial resolution. In this review, we focus on emerging methods for optical detection of neurotransmitter release and discuss fluorescent sensors/probes for monoamine neurotransmitters such as dopamine and serotonin. We focus on the latest advances in near infrared fluorescent carbon nanotube-based sensors and engineered fluorescent proteins for monoamine imaging, which provide high spatial and temporal resolution suitable for examining the release of monoamines from cells in cellular networks.

1. Biological background and motivation

Intercellular communication is a vital mechanism by which biological signals are transmitted between cells of a multicellular organism. The nervous system in particular is an example of complex intercellular communication and uses specialized structures to receive, process and send signals throughout an organism. Signals are propagated both within the nervous system, between specialized cells called neurons, and from the nervous system to cells in peripheral tissues such as skeletal muscle. The transmission of signals from a neuron to another cell is referred to as neurotransmission. Neurotransmission generally involves the secretion of a specific biomolecule, a 'neurotransmitter', from a stimulated neuron into the extracellular space (Figure 1a). The neurotransmitter then diffuses and activates postsynaptic receptors, communicating a chemical message from one neuron to its target cell. Classically, neurotransmission occurs at specialized structures called synapses, comprising a presynaptic bouton from which the neurotransmitter is released and a postsynaptic structure on the target neuron at which receptor proteins are concentrated (Figure 1a).

Within a neuronal presynaptic structure, neurotransmitters are stored in tens to thousands of highly concentrated small vesicles (in the 0.1 mol/L range) from which they are released through exocytosis milliseconds after stimulation of the neuron.[1,2] Neurons can form up to 350,000 individual synapses with other cells,[3,4] constructing complex neuronal circuits that give rise to the central nervous system and are capable of transmitting and computing huge volumes of information. These highly dynamic networks facilitate the function of the nervous system as the master controller and computer of the organism.

[a] M. Dinarvand, Dr. S. Kruss
Institute of Physical Chemistry
Göttingen University
Tammannstrasse 2, 37077 Göttingen (Germany)
E-mail: skruss@gwdg.de
[b] S. Elizarova, Dr. J. Daniel
Department of Molecular Neurobiology
Max Planck Institute of Experimental Medicine
37077 Göttingen (Germany)

There are hundreds of identified chemical transmitters in the central nervous system. Glutamate and GABA are the predominant fast-acting neurotransmitters, rapidly activating or inhibiting target neurons respectively. The majority of other neurotransmitters are modulatory, acting to modify neuronal activity on a slower timescale and exerting either excitatory or inhibitory effects on neurons in a context-dependent manner. One notable family of modulatory neurotransmitters is the monoamines, which includes dopamine, serotonin, norepinephrine, epinephrine and histamine. Monoamines also play an important role as hormones. For instance, epinephrine is secreted from adrenal medulla in response to sympathetic innervation and mediates a wide range of physiological response, broadly called fight or flight response.[5] Serotonin is secreted by enterochromaffin cells in the gastrointestinal tract and regulates intestinal motility and digestion.[6] Researchers have also reported the production and release of these molecules from cells even without neuronal innervation (Figure 1a). For instance, some immune cells are capable of production and release of neurotransmitters such as dopamine, to self-regulate or possibly communicate with other immune cells through autocrine and paracrine signalling to modulate immune responses.[7,8]

The mechanisms that control release and diffusion of neurotransmitters in the extracellular space are critical in intercellular communication. Thus, understanding the dynamics of neurotransmitter release has been an intense area of research over the last several decades. There are various factors regarding monoamine exocytosis that complicate studying the dynamics of release compared to other signalling chemicals. In the following section we will discuss some of those challenges and why they necessitate unique detection systems to observe release events with high spatial and temporal resolution.

Monoaminergic neurotransmission it thought to occur largely via volume transmission, meaning that following monoamine release from a presynaptic bouton, the monoamine diffuses in a relatively large distance and is able to act on receptors, and thus regulate the target cells over an area of up to several micrometers from the release site. diffusing monoamines can also be degraded by specialized enzymes or taken up into neighboring cells which limits the area that is affected by the monoamine.[9] For example, the half-life of dopamine in the striatum is ~30 ms, meaning that dopamine can potentially diffuse ~7 μm from a release site before degradation or

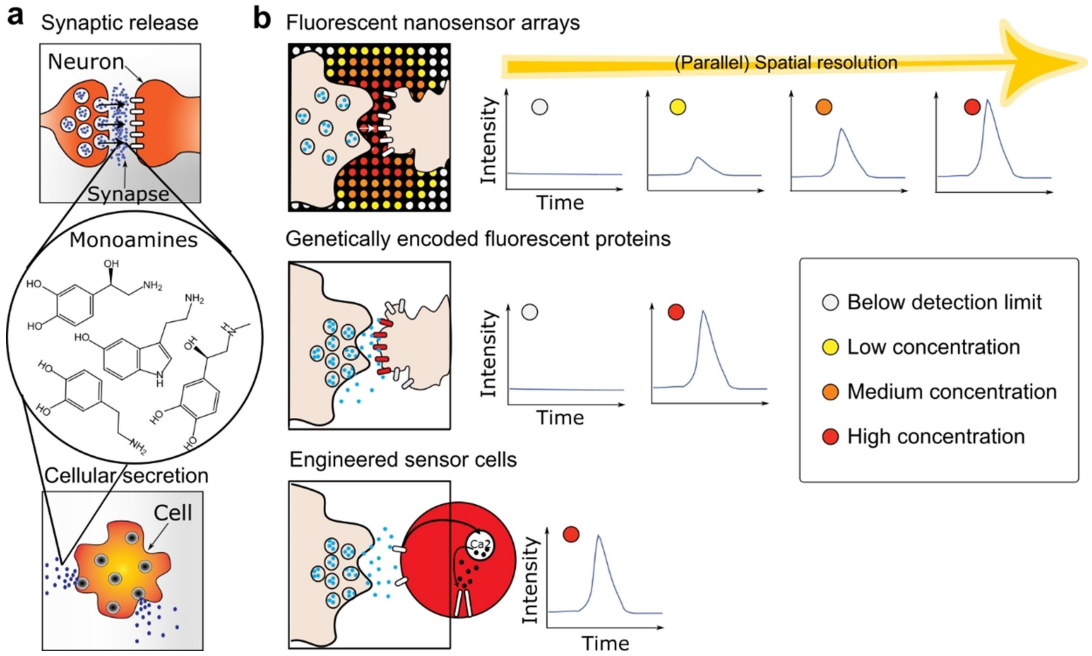

Figure 1. Monoamine detection by fluorescent sensors: **a**, Release of monoamines such as dopamine, epinephrine, norepinephrine or serotonin can occur at synaptic structures (synaptic transmission) of neurons or other release sites of monoaminergic cells. **b**, Optical methods to detect monoamines. Individual nanosensors are capable of reporting the local monoamine concentration through a transient change in their fluorescence. If there are many nanosensors ('array') in close proximity to the cell, they provide a very high spatial resolution (top panel). Genetically encoded sensors are fluorescent proteins that are expressed by cells on their surface and change their fluorescence in response to the analyte, providing information from the cell surface (middle panel). Cell-based sensors are engineered cells that undergo a fluorescence change on the level of the whole cell in response to the analyte. Due to the large size of these cells, this method provides lower spatial resolution (bottom panel). As indicated by schematic traces on the right of the panels, spatial and temporal resolution depends on the size, distribution and density of the sensor/probes and decreases from the top approaches to the bottom.

Meshkat Dinarvand earned her Doctor of Pharmacy degree from Tehran University of Medical Sciences in 2014. She has been working as a research assistant in the field of nanomedicine ever since, including at the nanomedicine and biomaterial lab in Harvard Medical School, Brigham and Women's hospital. She is now working toward her Ph.D. thesis at the Institute of Physical Chemistry, Georg August University of Göttingen. She is interested in designing nanosensors for biological applications with a focus on carbon nanotube-based sensors.

Sofia Elizarova received her B.Sc. degree in biology (University of Hannover) and M.Sc. degree in neurobiology (University of Göttingen) in Germany. Since 2017 she has been undertaking research for her Ph.D. in the Department of Molecular Neurobiology at the Max Planck Institute of Experimental Medicine, Göttingen, Germany, as part of the Göttingen Graduate Center for Neurosciences, Biophysics, and Molecular Biosciences (GGNB). Her current work focuses on the molecular mechanisms that regulate secretion of the neurotransmitter dopamine from presynaptic terminals.

Dr. Daniel completed his Ph.D. in 2008 with Prof. Bryce Vissel at the Garvan Institute of Medical Research (Sydney, Australia), examining presynaptic function in dopaminergic neurons. He then completed postdoctoral training with Prof Phillip Robinson (Children's Medical Research Institute, Sydney, Australia), discovering synaptic vesicle endocytosis inhibitors, and with Prof Nils Brose (Max Planck Institute of Experimental Medicine, Göttingen, Germany), investigating neuronal protein SUMOylation. In 2016, he established his own group within the Department of Molecular Neurobiology, focused on discovering mechanisms that regulate dopamine secretion.

Dr. Sebastian Kruss received his Ph.D. in physical chemistry at Heidelberg University and the Max Planck Institute for Intelligent Systems (Prof. Joachim Spatz). He then moved to the group of Prof. Michael Strano at the Massachusetts Institute of Technology, where he worked on carbon nanomaterials. Since the end of 2014 he heads an independent research group at Göttingen University. His research focuses on novel materials, spectroscopy and microscopy, biosensors and biophysics.

uptake.[10] Monoamine release sites are also highly heterogeneous.[11,12] A research investigating neurons that secrete dopamine has shown that presynaptic boutons are formed at various distances from target neurons, meaning that dopamine must diffuse away from the release site to bind to receptors on target neurons.[12,13] In addition, dopamine can be released not only from boutons but also from the cell body of neurons, which in the brain are located distant from boutons (Figure 1b).[14] The heterogeneity of release sites is unique to modulatory neurotransmitters and suggests that these neurons use distinct mechanisms for intercellular communication that are not yet understood.

These processes alter the local extracellular concentration of the neurotransmitter, and thus influence signal transmission and integration by other cells. This mode of action is substantially different from fast-acting transmitters such as glutamate and GABA, which are secreted within a nanometer-range from their target receptors in synaptic structures and have a very limited half-life in the extracellular space, limiting their diffusion.[15,16]

The study of monoamine release requires sensors that detect monoamines. Given the diversity of the structures that release monoamines, as well as the dynamics of monoamine release and diffusion in time and space, an ideal detection method would need both high temporal and spatial resolution.[17] To achieve high temporal and spatial resolution, optical monoamine detection methods are an elegant solution (Figure 1b). Figure 1 illustrates detection and imaging of monoamines that the three major classes of existing fluorescent sensors/probes can perform. Following a release event, the concentration of the neurotransmitter rapidly changes adjacent to the release site. The spatiotemporal detection limits for the secreted neurotransmitter are thereby determined by the distance between the sensor-probes as well as their kinetics and sensitivity (see section 3.1). Consequently, the spatiotemporal resolution of neurotransmitter detection can be improved by increasing the number of probes in close proximity to the cell, as well as the dynamic range of the probe and optimal kinetics.

This minireview provides a short overview of the classical analytical methods of monoamine neurotransmitter detection (Section 2), with a focus on dopamine and serotonin. We then review advances in fluorescent optical monoamine sensors: a) fluorescent nanosensors that are positioned outside cells, b) engineered fluorescent proteins expressed on the surface of cells, and c) whole cells as fluorescent monoamine sensors. We also provide a short summary of fluorescent probes and label-free methods, although the focus are the mentioned direct methods with high spatial and temporal resolution.

2. Classical methods of monoamine detection

The most extensively used analytical methods to detect monoamine secretion are microdialysis and electrochemistry.[18] Microdialysis is a procedure in which a sampling probe of approximately 0.15–0.3 mm is surgically implanted in the brain or tissue area of interest, such as the striatum of anesthesized rodents.[19] Extra-cellular fluid is then sampled by diffusion through a semi-permeable membrane at the tip of the probe with a constant flow rate of typically 0.5–5 μL/min. This procedure is combined with analytical tools such as liquid chromatography and mass spectrometry to determine the concentration of monoamines in the extracellular fluid. While enabling the investigation of deep areas of the brain with high chemical specificity *in vivo*, the relatively long sampling procedure (in order of minutes) and size of the probe does not allow monitoring of millisecond fluctuations in monoamine concentrations. The method is also relatively invasive and damages brain tissue due to the insertion of the sampling probe. Such a damage can induce an inflammatory response and thus introduce artefacts to the experimental system.[20]

The temporal and spatial resolution of monoamine detection was greatly improved by the development of the electrochemical methods such as amperometry and fast-scan cyclic voltammetry.[21–24] In amperometry, a carbon fiber microelectrode held at constant electrical potential is placed either adjacent to cells or in a brain area of interest. Monoamines oxidize at the electrode surface and yield faradaic current as the quantitative indicator of concentration.[25] Damage to brain tissue is reduced compared to microdialysis due to the relatively small probe radius (3.5 μm or much smaller).[26] One limitation of amperometry is the lower chemical resolution/selectivity as amperometry cannot distinguish between monoamines of similar redox potential (dopamine, epinephrine, and norepinephrine) and other molecules (e.g. ascorbate). Therefore, it is often used in cultured cells or brain slices in which contamination of the signal from other chemicals can be excluded. Nevertheless, due to the excellent temporal resolution on a submillisecond scale and the high sensitivity, amperometry has become the gold standard of monoamine detection and has been used to record single release events in cultured cells.[27–29] A subsequent methodological breakthrough was the adaptation of carbon fiber electrochemistry to yield voltammetry-based methods. Fast-scan cyclic voltammetry (FSCV) is widely used for the detection of monoamines *in vivo*, and works by cycling the potential of the electrode between a positive and negative voltage at high rates to rapidly reduce and oxidize the analytes. This results in cyclic voltammograms with characteristic shapes for individual compounds, resulting in greater discrimination of analytes but greatly reduced temporal resolution compared to amperometry.[29]

While electrochemical methods can provide exquisite temporal resolution, they provide very limited (parallel) spatial resolution. Differentiating sub-cellular release structures or even release from single cells using brain slices or dissociated neuron cultures has proven to be extremely challenging due to the high density of release sites and relatively large size of the carbon electrode.[27] One strategy to overcome these limitations is using multi-electrode arrays containing 64 microelectrodes with electrode diameters of 3 μm to 12 μm, however this method is limited to use in cell culture.[30]

3. Fluorescent sensors based on nanomaterials

In general, a fluorescent nanosensor is composed of a nanoscale fluorescent material and equipped with recognition chemistry to bind an analyte. Structures on the 'nanoscale' (in the range of 1–100 nm in at least one dimension[31]) often acquire novel size and shape dependent optical properties that are not present in the bulk material.[32] An important property is emission in the near infrared (nIR) tissue transparency window (> 800 nm) that only few fluorophores such as carbon nanotubes, certain silicate nanosheets or quantum dots provide.[33–35] These size-dependent properties, coupled with tailored surface chemistry make fluorescent nanomaterials sensitive and versatile sensors for biological applications down to the single-molecule level.[36,37] Furthermore, fluorescent sensors can be detected by non-invasive imaging techniques, which provide high parallel spatial resolution (increased spatial resolution without reducing the field of view). Many nanoscale structures have been studied as detection tools for neurotransmitters, including fluorescent complexes, metallic, polymeric and carbon-based materials. These tailored materials report the presence of the analyte in a biological sample and include quantum dots,[38] graphene,[39] and polymeric nanoparticles.[40] However, they do not all provide spatiotemporal information such as dynamic information of individual release events from cells. In this review, we will focus only on (fluorescent) nanosensors that have successfully visualized release dynamics in a biological system with appropriate temporal and spatial resolution in addition to chemical resolution. In Section 3.1, we will shed light on the kinetic requirements for monoamine imaging. Then, SWCNT-based fluorescent sensors for dopamine and serotonin are discussed (Section 3.2). Finally, polymer nanoparticle approaches will be addressed (Section 3.3).

3.1 Kinetic requirements for fast imaging of neurotransmitter release

In standard analytical techniques, detection of an analyte occurs under equilibrium conditions in which the concentration of the analyte is constant. In this scenario, the binding affinity/limit of detection of the detection system is the most important parameter. In contrast, many biological processes such as neurotransmitter release are characterized by fast concentration changes (ms time scale) and complex spatiotemporal patterns. These patterns are governed by release events, diffusion and uptake. For example, studies have shown that most dopamine receptors (D1 and D2) in the striatum are extra-synaptic.[41] This means that dopamine spills over from the release site to reach its many target receptors. At short distances from the release site (1–2 μm), only diffusion governs the extent to which the DA signal spread through the extracellular space. However, in the range of 5 to 20 μm from the release site, uptake of dopamine limits dopamine concentration.[16] For example, a study has shown that if each vesicle contains 3000 molecules, dopamine would diffuse and bind to dopamine receptors in an area of 12 μm however, when dopamine transporters (DAT), responsible for dopamine uptake from the extracellular space, are missing such as in Parkinson's disease, the diffusion distance of the dopamine precursor L-DOPA may be as high as 32 μm.[42] These considerations show that secreted monoamine concentration is a complex function of location (x,y,z) and time.

When imaging such highly complex processes with fluorescent sensors, the kinetics of these sensors determine the resolution that can be achieved. To study the relation between kinetics and resolution Meyer *et al.*, developed a theoretical framework to simulate the image of many single fluorescent sensors when exposed to concentration changes of analytes (e.g. neurotransmitters) released from cells.[43] It is not only valid for nanomaterial-based sensors but for every immobilized/bound fluorescent sensor/probe on or around a cell.

For this purpose, a stochastic kinetic Monte Carlo simulation was implemented and sensors/probes with a certain number of binding sites and rates of binding and unbinding were modelled. As a typical biological scenario, a cell releasing molecules via exocytosis and diffusion through space was used and simulated (Figure 2a). The approach also considered the resolution limit of light microscopy as well as technical aspects such as the imaging speed. This simulation was then used to calculate if a given sensor (array) with certain forward (k_{on}) and backward rate constants (k_{off}) can e.g. distinguish two release events in time or distinguish multiple release sites. Figure 2b shows the concentration profile of a typical single exocytosis event and images of different sensor arrays at different time points. The results show that certain sensors cannot detect the release event while others oversaturate. By simulating many different rate constant combinations it was possible to explore this rate constant design space. Interestingly, sensors with rate constants of $k_{on} = 10^6\ M^{-1}s^{-1}$ *and* $k_{off} = 10^2\ s^{-1}$ provide the best spatiotemporal resolution for many scenarios. This means that nanosensors with relatively low binding affinity ($K_d = k_{off}/k_{on} = 100\ \mu M$) exhibit the best response profile. At slower binding rates ($k_{on} = 10^3\ M^{-1}s^{-1}$) release events cannot be detected and at faster binding rates ($k_{on} = 10^7\ M^{-1}s^{-1}$) and slow unbinding ($k_{off} = 1\ s^{-1}$) the response quickly saturates (Figure 2b). These insights are important for the design of monoamine sensors but provide also the tools to analyze data acquired with such sensors and address the inverse problem, i.e. translate an image into a concentration profile.

3.2 Carbon nanotube-based nanosensors

3.2.1 Concept and design of SWCNT-based nIR fluorescent sensors

Carbon based nanomaterials hold a unique position in life science research due to their physicochemical properties (i.e., optical properties, electrical conductivity, mechanical strength, thermal properties).[44] Nano structures based on carbon have been studied extensively as sensors. Among them, the most promising structures are carbon dots, graphene, and carbon nanotubes.[36,45]

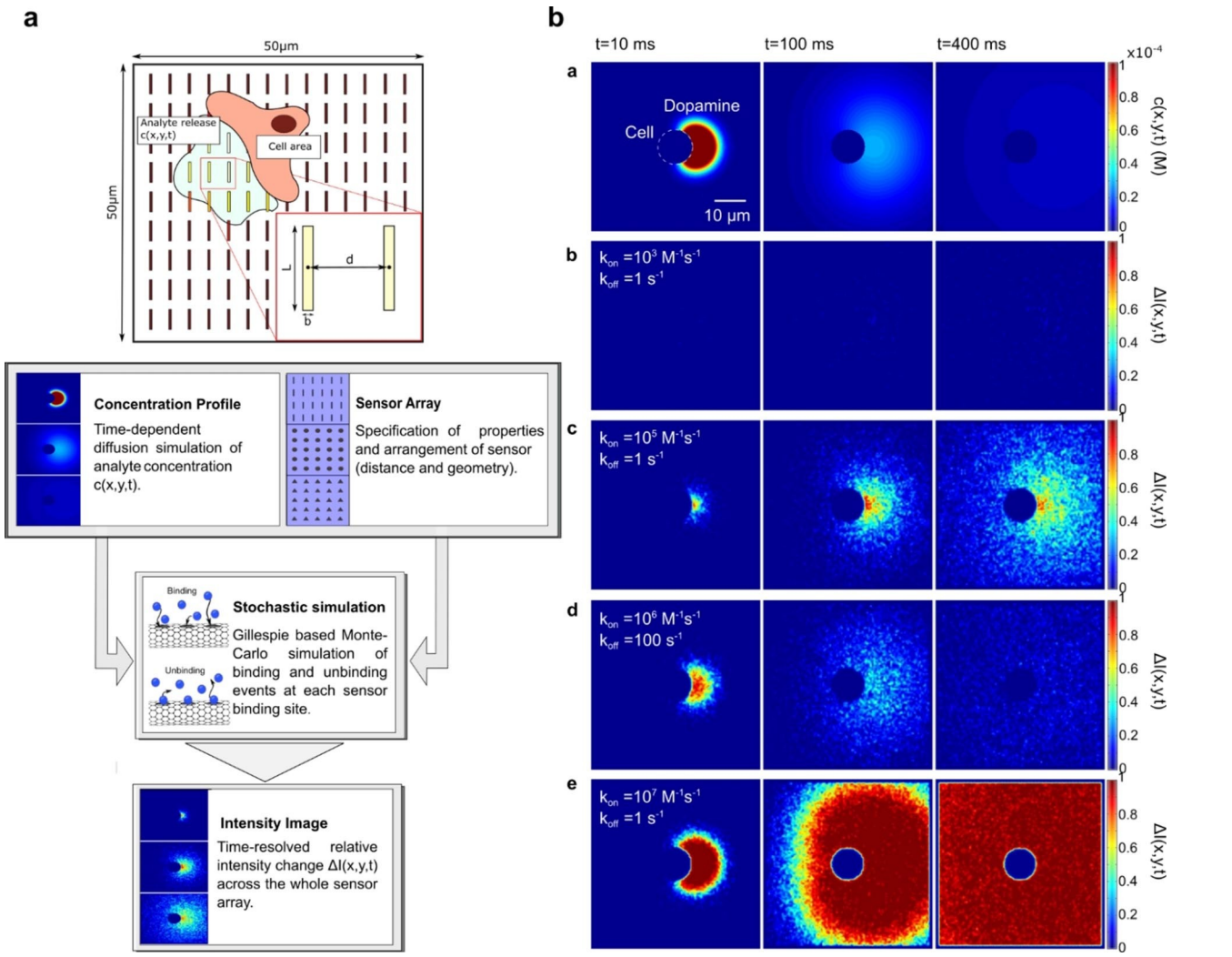

Figure 2. Kinetic requirements for sensors that enable high spatiotemporal resolution imaging. **a**, Model of a surface coated with nanoscale sensors. A cell on top releases a molecule of interest exposing the array to a certain concentration profile c(x,y,t). Bottom: Flow diagram of the simulation: (1) Simulation of neurotransmitter release from a cell and diffusion. (2) Arrangement of the sensors in any arbitrary geometry and size. (3) Stochastic simulation of binding and unbinding events of the analyte to the nanosensor with different rate constants k_{on} and k_{off}. (4) Finally, the image series $\Delta I(x,y,t)$ is calculated by overlaying the fluorescence intensity point spread functions of all sensors and accounting for the resolution limit of light microscopy (Abbe limit), pixel size, and frame rate of the detector. **b**, Fluorescence changes of nanosensors in response to dopamine release from a cell (top row) All other rows: Simulation of fluorescence changes of a nanosensor array after neurotransmitter release from a vesicle at different time points for different k_{on} and k_{off}. The differences show the importance of rate constants for the spatiotemporal resolution and the observed response pattern. Adapted from reference [43] with permission. Copyright 2017 American Chemical Society.

Single walled carbon nanotubes (SWCNTs) can be imagined as rolled up sheets of graphene.[46] Because of their small diameter (e.g. 0.7 nm) and high length, they can be conceived of as one-dimensional materials. The angle and the direction in which the graphene sheet is 'rolled up' determines distinct lattice structures called chirality and is described by the chiral index (n,m). The special lattice structure causes very unique optical, mechanical and electrical properties. For instance, semiconducting SWCNTs are fluorescent in the near infrared (nIR) region (>850 nm).[33] Their electronic band gap structure and nIR emission wavelength depends on the chirality of carbon nanotubes.[33] For example, (6,5)-SWCNTs emit at around 980 nm while (7,6)-SWCNTs emit at around 1130 nm.

Intrinsic fluorescence in the near infrared region and the ability to manipulate the fluorescence emission patterns, is the basis of optical sensing with SWCNTs.[33,36] SWCNTs, unlike most organic fluorophores, do not photobleach or blink. Furthermore, SWCNT-based sensors can be designed specifically to resist biofouling which is one limitation of microelectrode-based sensors.[47] Fluorescent SWCNTs are especially advantageous for biomedical imaging because of the nIR fluorescence in the tissue transparency window, which could potentially facilitate through-cranium imaging.[48] In the nIR, there is little light absorption by tissue, relatively low light scattering and minimal autofluorescence.[49] Therefore, this spectral range is desirable for biomedical imaging. The fluorescence of SWCNTs is highly sensitive to its environment, meaning small changes in

the SWCNT's microenvironment can affect their fluorescence emission pattern. However, SWCNTs are extremely hydrophobic and therefore not stable in aqueous solutions. In order to use SWCNTs in biological applications, they must be functionalized to facilitate colloidal stability. Additionally, surface modification can be used to purify chirality enriched SWCNTs.[50] Non-covalent surface modification with DNA, peptides, proteins and other polymers have been extensively used to tailor the surface chemistry on SWCNTs.[51–55]

SWCNTs have been used as building blocks for sensors and labels for larger biomolecules such as RNA, DNA and proteins.[53,56–59] For smaller analytes, it is typically difficult to find good recognition units and therefore designing sensors is more challenging. One approach is indirect sensing of the analyte by detecting the product of the analyte's chemical reaction. An example is SWCNT H_2O_2 sensors equipped with hemin that catalyzes the reaction of H_2O_2 to hydroxyl radicals, which directly quench fluorescence and this indicates the presence of the signalling molecule H_2O_2.[60] This concept is only feasible for a few reactive/quenching compounds. Interestingly, certain biopolymer wrapped SWCNTs can detect small molecules such as dopamine with high sensitivity and selectivity, even without a known recognition unit (Figure 3a).[50,61–63] This phenomenon was termed corona phase molecular recognition.[61] Similar to antibody-antigen recognition, the molecular recognition relies on the spatial arrangement of the polymer on the SWCNT with a specific 3D structure that binds dopamine. One important class of macromolecules for SWCNT modification is single stranded DNA (Figure 3b). As shown in Figure 3, the baseline fluorescence of certain DNA wrapped SWCNTs increase dramatically when they are exposed to dopamine either in dispersion (Figure 3b) or immobilized on a surface (Figure 3c). Furthermore, the fluorescence increase is concentration dependent (Figure 3d).

Whether a DNA functionalized SWCNT responds to dopamine depends on the DNA sequence.[61] The first identified and studied sequence was $(GT)_{15}$ ssDNA on HiPCo SWCNTs. The fluorescence of $(GT)_{15}$-SWCNTs increased by 80% in solution and up to 400% on the single SWCNT level after addition of dopamine (100 μM). The dynamic range of detection was 10 nM - 10 μM and the limit of detection was 11 nM.[61] To improve sensitivity and selectivity, the DNA sequence was further explored. Consequently, a study with (6,5) chirality enriched SWCNTs with 10 ssDNA sequences was performed to identify which DNA sequence imparted highest sensitivity and selectivity to dopamine compared to other catecholamines (epinephrine and norepinephrine).[62] All sequences responded to the catecholamines with an increase in fluorescence signal. However, there was a marked difference in analyte selectivity between different ssDNA sequences (Figure 4). For example,

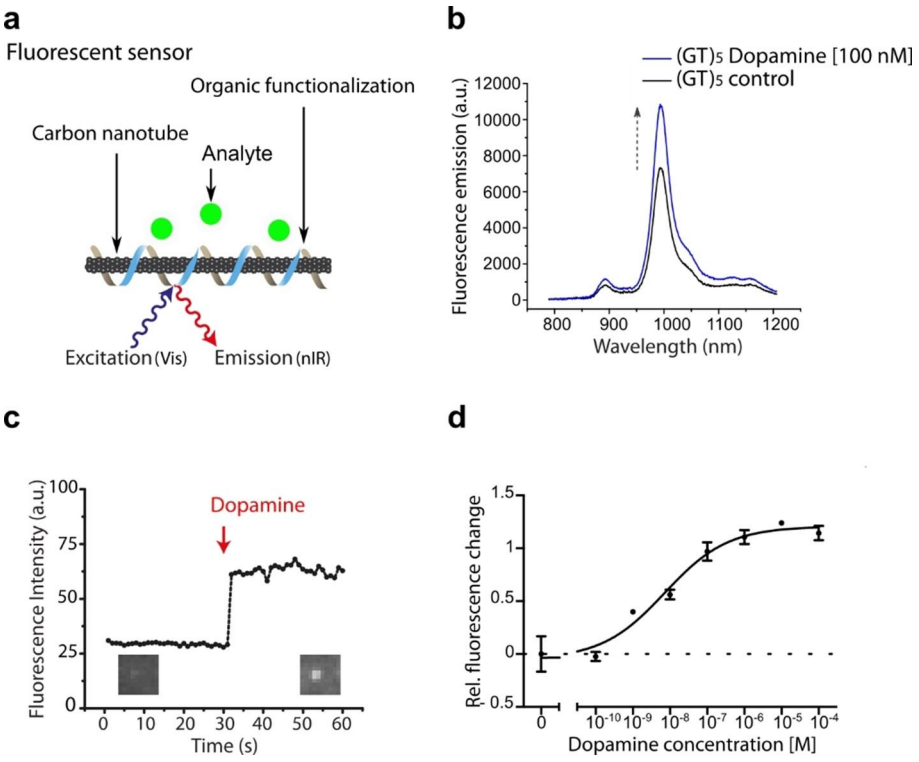

Figure 3. Carbon nanotube-based near infrared fluorescent sensors for dopamine. **a**, Schematic of a functionalized single-walled carbon nanotube (SWCNT) sensor. In presence of the analyte, the nIR fluorescence changes. **b**, Fluorescence emission spectra of $(GT)_5$ DNA functionalized (6,5) single chirality SWCNTs before (black) and after (blue) addition of dopamine show an increase in fluorescence intensity. **c**, nIR fluorescence intensity of a single SWCNT sensor immobilized on a surface. A sharp increase in fluorescence is observed after addition of dopamine. **d**, Calibration curve of a SWCNT-based dopamine sensor shows nM sensitivity. (**a**) and (**b**) adapted from references [61] and [64] with permission. Copyright 2014 and 2019, respectively, American Chemical Society. (**c**) adapted from reference [65] with permission. Copyright 2017 United States National Academy of Sciences, (**d**) adapted from reference [62] with permission. Copyright 2017 MDPI.

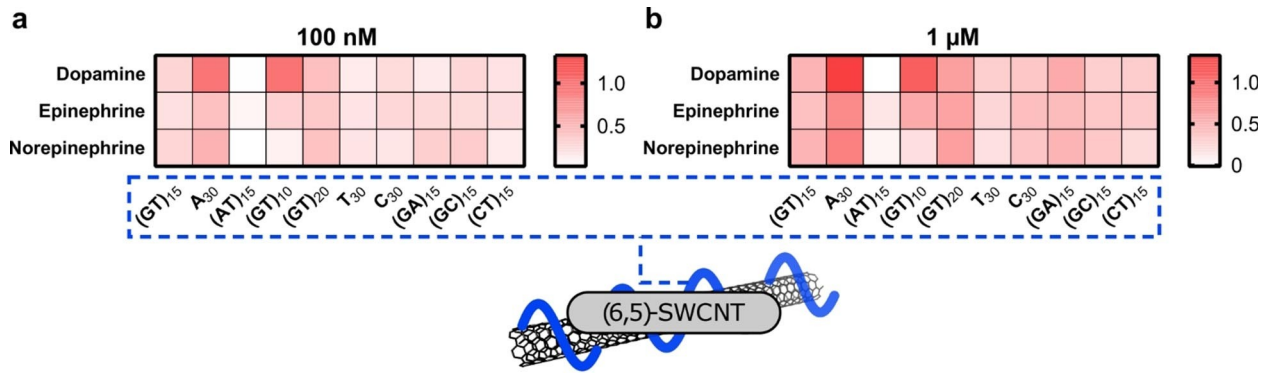

Figure 4. Tuning of SWCNT-based dopamine sensors by exploring the DNA sequence space. Fluorescence intensity changes of various DNA functionalized SWCNTs at **a**, low (100 nM) and **b**, high (1 µM) catecholamine concentrations. These results indicate e.g. that $(GT)_{10}$-SWCNTs can discriminate to a certain extent different catecholamines. Reproduced from reference [62] with permission. Copyright 2017 MDPI.

$(GT)_{10}$-SWCNTs showed the highest selectivity and sensitivity for dopamine (table 1). K_d values of $(GT)_{15}$ and $(GT)_{10}$-SWCNT sensors ranged between 395.2 and 9.2 nM respectively. In light of the relevance of kinetics and off-rates for imaging (see previous section) it is crucial that kinetics of a sensor and the required resolution for a specific biological question match. Therefore, a sensor with the highest sensitivity is not necessarily the best fit for a biological experiment. Most dopamine sensors were so far created by using non-purified SWCNTs. Multiplexing approaches have a huge potential and therefore chirality-pure sensors are desired. A recent study used corona phase exchange purification (CPEP) to isolate chirality pure (6,5)-SWCNTs to coat them with e.g. $(GT)_5$DNA.[50] The results show that dopamine sensing can be as well performed with purified SWCNTs and well-defined emission features can be obtained (see also figure 3b).

In summary, functionalization of SWCNTs with specific DNA sequences leads to highly sensitive dopamine sensors. The enormous potential sequence space promises many additional discoveries and improvements for the future. One might even speculate that folding of biopolymers such as DNA on a SWCNT could be a generic approach to create recognition motifs.[66]

3.2.2 Mechanism of fluorescence modulation

The mechanism of SWCNT-based fluorescent sensors is an active area of research and might vary between different surface chemistry approaches and analytes. However, for DNA-SWCNT-based dopamine sensors there have been insights that are of general importance for the field.

The first insights into the recognition and sensing mechanism were gained by coating SWCNTs with a fluorophore tagged $(GT)_{15}$ DNA. Initially, adsorption of tagged DNA on SWCNT surface quenched the fluorophore's visible fluorescence. When dopamine was added, this fluorescence increased again.[61] The best explanation is that the fluorophore moved away from the SWCNT, which recovered its fluorescence that had been quenched by the proximity of the SWCNT. This finding suggests that a conformational change might be responsible for the change of nIR fluorescence.

However, dopamine and other catecholamines are redox-active compounds. Therefore, one could also hypothesize that increase in fluorescence is linked to this property, especially as certain reducing compounds are known to increase nIR fluorescence.[67] However, the extent of fluorescence change depends on the nature of the polymer wrapping as shown in Figure 5a.[63] Therefore, the redox potential of the analyte alone cannot be the only reason responsible for the fluorescence response to dopamine. This is further supported by the fact that several compounds of the same redox potential as dopamine do not show this characteristic fluorescence increase. Another possible explanation is electron transfer from dopamine to the DNA phase. Again, a mechanism based solely on electron transfer is unlikely because the dopamine response is reversible. As discussed earlier, selectivity and sensitivity of

Table 1. Dissociation constants (K_d) and limits of detection (LOD) values of various DNA functionalized SWCNTs for catecholamines. Reproduced from reference [62] with permission from MDPI.

	NT	$[GT]_{15}$	$[GT]_{20}$	$[GT]_{10}$	A_{30}	C_{30}	T_{30}	$[GA]_{15}$	$[GC]_{15}$	$[C]_{15}$	$[AT]_{15}$
K_d (nmol/L)	D	395.2[a]	42.3	9.2	28.4	499.2[a]	237.2	627.8[a]	0.7[a]	25.8	9438
	E	159.1	112.6	178.2	171.9	177.2	51.1	234.3	49.3	47.1	241.5
	N	70.3	58	71.9	25	193.1	33.6[a]	21.4	2.3	52.8	-[1]
LOD[b] (nmol/L)	D	6.4[a]	0.6	0.1	3.6	2.7[a]	1.2[a]	507.2	28.5[a]	4.4	3776.6
	E	1.4	2.2	0.7	3.2	1.4	1.0	1.8	0.5	0.8[1]	23.7
	N	3.2	2.4	7.7	1.6	4.8	33.3	3.8	0.5	3.9	[1]

[a] No clear (sigmoidal) fit possible. [b] LOD: Limit of detection definition used = 3x standard error at [c] = 0 nM. D: Dopamine. E: Epinephrine. N: Norepinephrine.

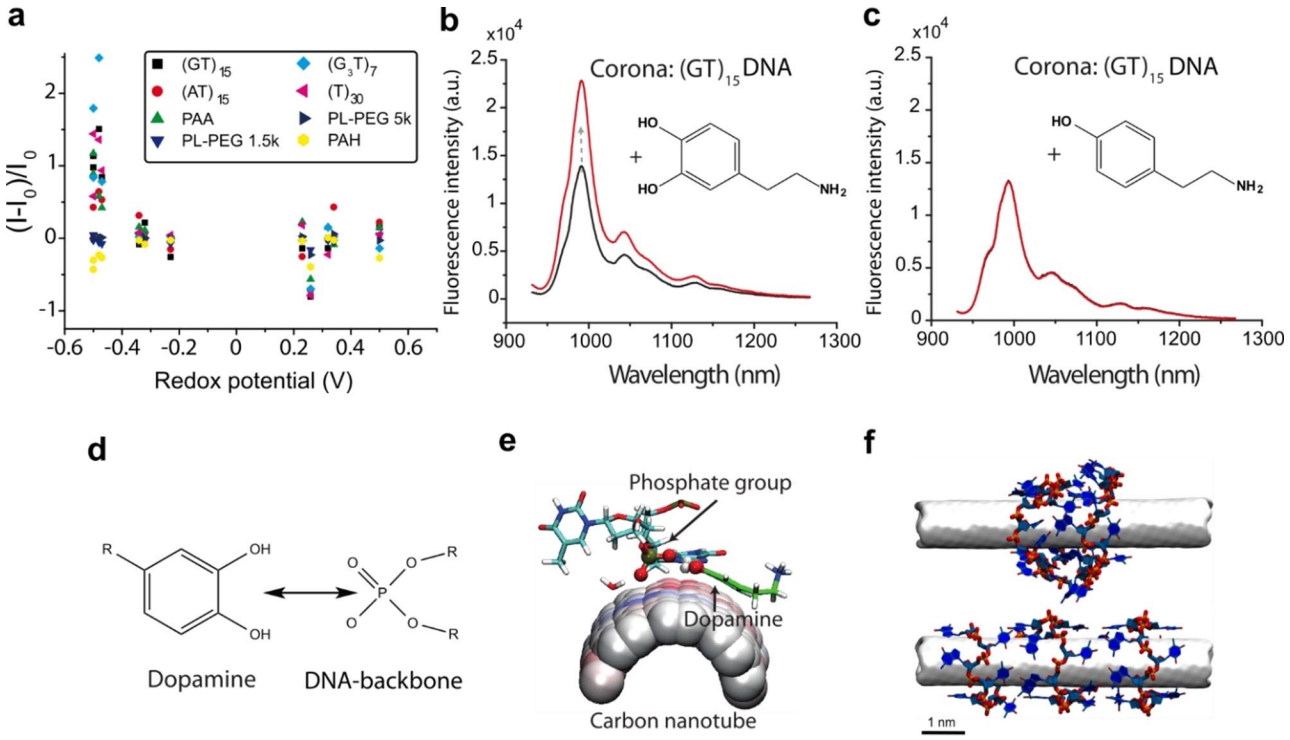

Figure 5. Mechanism of DNA-SWCNT based dopamine sensors. **a**, Fluorescence changes of SWCNT wrapped with various polymers when exposed to redox active molecules show a broad distribution, which cannot be explained by redox potential. **b,c** Fluorescence response of $(GT)_{15}$-SWCNTs to dopamine (a) and tyramine (b) before (black) and after (red) addition. The results show that small differences in the analyte structure completely change the response. **d,e**, Dopamine and adsorbed DNA on the SWCNT most likely interact via the phosphate backbone and hydroxy groups. **f**, MD simulations of DNA adsorbed on SWCNTs show that the DNA molecules do not form perfect helixes around SWCNTs (top) and stack on each other when experimental numbers of surface coverage are used. In contrast, without any constraints in the simulation helical structures are formed (bottom). (**a**) reproduced from reference [63] with permission. Copyright 2016 American Chemical Society, (**b**-**e**) reproduced from reference [65] with permission. Copyright 2017 United States National Academy of Sciences, (**f**) reproduced from reference [64] with permission. Copyright 2019 American Chemical Society.

sensors depend on the sequence of DNA strands absorbed on the surface. This shows that the interaction between the DNA and SWCNT plays an important role in the molecular recognition and formation of the fluorescence response. The surface area of the SWCNT that is covered by DNA molecules and the colloidal stability of the corona are parameters that likely define how the sensors detect dopamine. Therefore, the number of adsorbed ssDNA molecules was determined using an absorption spectroscopy based approach.[64] When H_2O_2 and riboflavin were used as analytes, the fluorescence response was directly proportional to the number of absorbed ssDNA molecules. However, no simple correlation was discovered between the fluorescence response for dopamine sensors, indicating that conformational changes of the DNA play a key role.[64]

Molecular dynamics (MD) simulations can provide insights into interactions between the analyte, the SWCNT and the organic phase. For $(GT)_{15}$-SWCNT, interactions between the hydroxy groups of dopamine and the phosphate groups of the DNA appear to play an important role (Figures 5d, e).[64] Due to these interactions, the phosphate groups move closer to the surface of the SWCNT and change the potential landscape through which the exciton diffuses. It is also possible that these conformational changes are associated with changes in ion distribution that are known to affect SWCNT fluorescence.[65] Experimentally, this interaction is validated because only dopamine homologues with two hydroxy groups show similar responses.[65] In contrast, tyramine (one hydroxy group) does not induce any fluorescence change (Figures 5b, c). One should also consider that the structure of DNA on SWCNTs is likely more complex with stacked nucleotides, as recently shown using experimental surface coverage parameters for MD simulations (Figure 5f).[64]

All mechanistic insights suggest that DNA acts as a flexible quantum yield switch on SWCNTs. For certain DNA sequences, the interaction with an analyte such as dopamine changes the conformation of the DNA, which in turn changes the quantum yield by affecting the exciton fate. Nevertheless, conformational changes due to unspecific changes in microenvironment would cause background signals and decrease selectivity. Therefore, more rigid xeno nucleic acids can be used to stabilize the fluorescence signal in media of different ionic strengths.[68]

3.2.3 Imaging dopamine release

A nanomaterial that changes its fluorescence in the presence of an analyte such as dopamine is a powerful tool for direct chemical imaging. Even though a single nanosensor responds to dopamine (Figure 3c), imaging many of them at the same time substantially increases the parallel (spatial) resolution.[65] For *in vitro* cell studies such sensors can be immobilized on a surface (sensor array) and cells cultivated on top (Figure 6a).

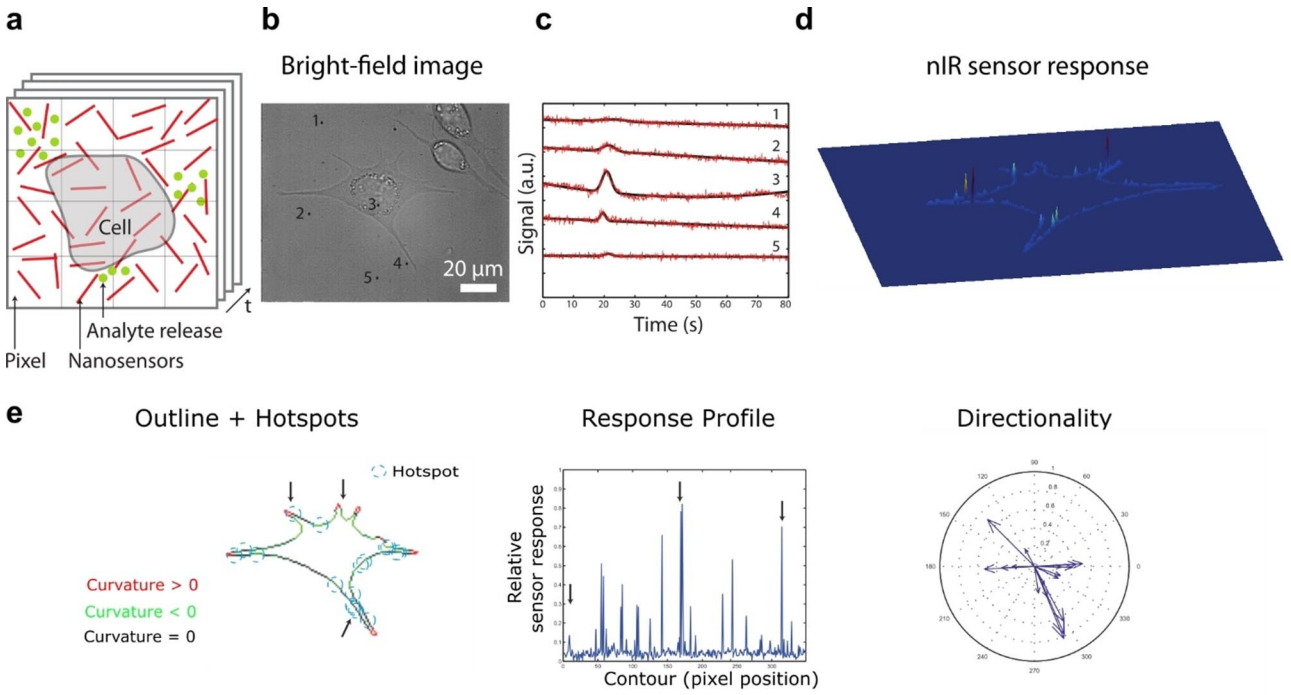

Figure 6. Fast imaging of dopamine release from cells using nanosensors **a**, Schematic of nanosensors immobilized in proximity of cells (like an array). **b**, Brightfield image of a neuroprogenitor PC12 cell incubated on top of a glass surface coated with SWCNT nanosensors. **c**, Fluorescence signal of dopamine nanosensors under and around this cell plotted against time. The differences in the traces show the gain in spatial information by imaging many nanosensors in different locations. **d**, Color-coded maximum responses (at the border) of the same cell showing localized events, denoting hot spots of neurotransmitter exocytosis/release. **e**, Localization of such hotspots around the cell and corresponding cell curvature. Additionally, the same information in directionality plots, which show that hotspots are located along cell protrusions preferentially in regions of negative curvature. Adapted from reference [65] with permission. Copyright 2017 United States National Academy of Sciences.

Above a certain sensor density the resolution limit of light microscopy becomes relevant and therefore the camera does not detect individual sensors anymore but the overlay of many of them. The above mentioned $(GT)_{15}$-SWCNT sensors and modified versions of it were used in this way to study dynamics of dopamine release from PC12 cells (a model cell line for modulatory neurotransmitter studies) (Figures 6a, b). Figure 6c shows the fluorescence trace of different regions under a cell (figure 6b) during stimulation with potassium, which triggers exocytosis through depolarisation of the cell membrane. The traces show peaks, which indicate increases of the dopamine concentration. The shapes and magnitudes of these traces vary across different regions, which highlights the high spatial resolution of the method (Figure 6c). The heterogenous distribution of maximum responses along the cell membrane is indicative of hotspots of dopamine release. These sensor arrays provide a great deal of temporal and spatial information from single cells, which is a key advantage of this method of dopamine detection. For example, when images are divided to units of 4×4 pixels, a round cell contains approximately 1700 reporter pixels (d = 40 µm) and more than 180 reporter pixels in a 2 µm zone around the cell border. These numbers highlight the gain in spatial resolution compared to electrode-based methods, which generally employ only a single sensor and at most have been able to employ 64 sensors in an electrode array.[30] In Figure 6, the nanosensors were imaged at 100 ms per frame, which is a lower temporal resolution than amperometry but comparable to FSCV. However, the time resolution was mainly limited by the imaging setup and could be further improved by 1–2 orders of magnitude.

SWCNTs are also useful for biomedical research in tissue samples. For example, single polyethylenglycole functionalized SWCNTs can be tracked in brain tissue to map the extracellular space.[69] Along the same lines, a variant of the above mentioned SWCNT-based dopamine sensor has been used to investigate dopamine release in brain slices of mice dorsal striatum,[70] which contains abundant sites of dopamine release, as it receives extensive axonal projections from dopaminergic neurons residing in the ventral midbrain.

To date, SWCNT-based dopamine nanosensors were either immobilized in arrays under cells or bound/diffused non-specifically in tissue samples. To target SWCNTs directly to specific locations such as a presynaptic structure, tailored sensors with recognition motifs are necessary. One approach is to additionally conjugate nanobodies to the DNA around the SWCNTs.[58] This approach did not affect dopamine sensing and opens up many opportunities to target such sensors specifically to the most relevant biological locations. Another approach to target dopamine nanosensors to specific locations was to make use of cells to transport them. Recently, it was shown that immune cells can be programmed to take up SWCNT-based dopamine sensors and transport them to desired locations where they are released.[71] After release, they are still functional

and detect dopamine, which promises interesting *in vivo* applications.

The sensors discussed in this section were identified *de novo* in a screening approach but in general it is faster to synthesize new sensors by relying on known recognition motifs such as antibodies, nanobodies or aptamers. In the next section, a sensor for the neurotransmitter serotonin will be discussed that is based on a DNA aptamer specific for serotonin.[72]

3.2.4 Imaging of serotonin release

Like dopamine, the local changes of serotonin concentration around neurons are responsible for signal transmission in neural circuits. Therefore, to better understand intracellular signalling by serotonin in the brain and other organs, chemical sensors with high spatial and temporal resolution are required. Again, there are very few (optical) methods that could provide high spatiotemporal resolution and visualize release events *in situ* with minimal invasiveness.

One approach to detect serotonin is the use of organic dyes that change their fluorescence when they react with serotonin, such as coumarin-3-aldehyde. This serotonin binding turn-on fluorophore can be used as a labelling agent to visualize serotonin rich vesicles inside cells and further image the dynamics of vesicular transport of serotonin upon cell secretion.[73] Even though this dye is relatively selective for serotonin, the dissociation constant is quite high ($K_d = 2400\ \mu M$). Therefore, this molecule is more suitable for detecting and imaging the presence of serotonin rather than studying dynamic changes in serotonin levels.

The first nIR fluorescent sensor for serotonin is based on SWCNTs (NIRSer).[72] It consists of (6,5)-SWCNTs that were non-covalently coated with a serotonin-specific DNA aptamer (Figures 7a). In the presence of serotonin, the nIR fluorescence increases (Figure 7b). Consequently, it can be used to image serotonin release from cells. Most of the serotonin in a human body is stored in blood platelets. Therefore, NIRSers were used to image secretion of serotonin from platelets with high spatial and temporal resolution (Figure 7c). By coating surfaces with NIRSers, and seeding adherent platelets on top of the sensors, the release hotspots (localized regions where exocytosis and serotonin release occurs) on the cell membrane were identified (Figures 7d, e, f). NIRSer has a dissociation constant (K_d) of 301 nM and is selective for serotonin compared to potentially interfering substances such as tryptophan. Again, the major advantage is the high spatial resolution. Using this approach, single cells can be studied in detail as well as cell populations.[72] In this context, the heterogeneity of serotonin release patterns, including onset and magnitude of serotonin release, was described for the first time in human platelets.

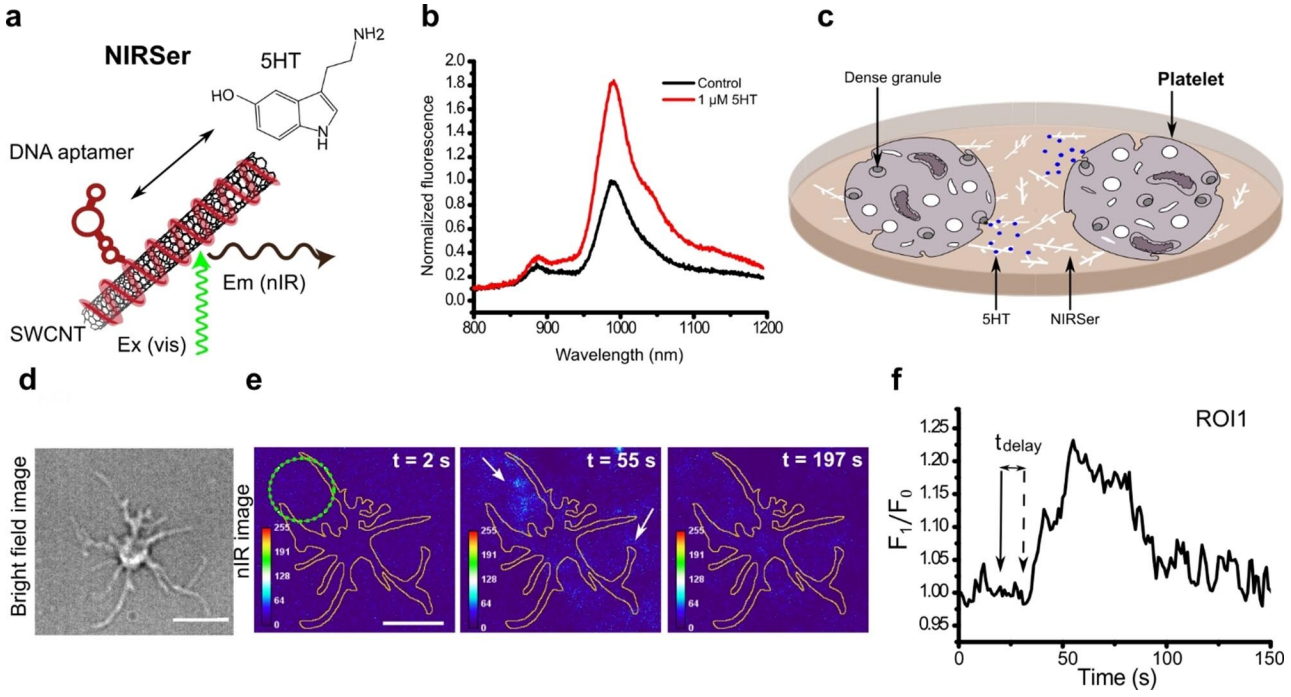

Figure 7. Near infrared fluorescent nanosensors for serotonin (NIRSer). **a**, Binding of serotonin to a serotonin- aptamer functionalized SWCNT leads to a change in aptamer conformation and, consequently, to an increase in the fluorescence of the SWCNT. **b**, Fluorescence spectrum of the nanosensor before and after addition of 1 μM serotonin showing 80% increase in fluorescence intensity. **c**, Schematic of how nanosensors and platelets were interfaced. Following platelet activation, serotonin is released and detected by the sensors. **d**, Bright field image of a single platelet adhered to a nanosensor coated surface. **e**, Color-coded nIR fluorescence images of the platelet in (e) before, during and after serotonin release. **f**, Fluorescence response from a ROI on the cell membrane showing a hotspot of serotonin release on the cell membrane, (green circle in image **e**). The scale bars are 5 μm. Adapted from reference [72] with permission. Copyright 2019 American Chemical Society.

3.3 Polymer-based nanosensors

Polymer based fluorescent sensors have an intrinsically versatile structure. Most polymers used as sensors in biomedical applications are biocompatible and biodegradable. Furthermore, various recognition units can be covalently or non-covalently attached to the polymer backbone to amplify the fluorescent signal or enable multiplexing.[74] For instance, several recognition units can be introduced in one nanosensor to increase the signal and sensitivity. One example, is a polymeric nanoparticle that was designed with fluorescent copolymers of fluorene and benzothiadiazole conjugated to phenylboronic acid units as dopamine recognition units. The advantage of this system is that each nanoparticle can have multiple dopamine binding sites. The sensing mechanism is most likely due to dopamine-induced fluorescence quenching. These fluorescent nanoparticles are biocompatible, selective for dopamine and have been successfully used in zebrafish embryos or larvae.[75] The nanoparticles were taken up by cells, making the system suitable for directly labelling cells that contain dopamine. However, they cannot be applied as an efficient sensor to image dopamine release dynamics at high spatial resolution and to monitor signal transmission through dopamine secretion.[75]

Polymers and polymer-coatings are widely studied in order to increase biocompatibility of nanoparticles or improve systemic circulation of the particles while avoiding detection by the immune system. For example, spherical nanoparticles with lipophilic core polymers and a biocompatible hydrophilic coating detected histamine *in vivo*.[76] In this sensor, an amine binding ionophore binds histamine molecules to the core polymer, which changes the local pH and decreases the fluorescence of a pH sensitive fluorophore ($K_d = 1.9$ mM). This nanosensor enabled *in vivo* detection of histamine injections. While the plasma concentration of histamine is around 8 μM, mast cells contain compartments with 100 to 500 mM histamine, leading to high localized histamine concentrations during inflammatory processes. Therefore, such sensors would be useful to detect and image inflammatory processes in tissue.

4. Genetically encoded sensors

An alternative to external sensors is genetically encoded sensors, which are introduced into cells as genetic material. The introduced genetic material causes cells to produce proteins that facilitate a measurable response to dopamine, such as an increase in protein fluorescence. Such sensors are highly suitable for *in vivo* investigations, since the gene encoding a given sensor can be incorporated into the host genome. Sensor expression is therefore non-invasive, and genetic techniques allow for targeted expression in subpopulations of cells, such as neurons. Such approaches can take two forms: cell-based sensor systems and protein-based sensor systems.

A cell-based fluorescent sensor was designed by Muller *et al.*,[77] named cell-based neurotransmitter fluorescent engineered reporters (CNiFERs). For this purpose, HEK293 Cell lines were genetically engineered to express D2 dopaminergic receptors coupled to G_q proteins to trigger an intracellular calcium increase upon binding to dopamine. A FRET-based calcium indicator was also genetically encoded in the cells. Thus, when dopamine binds to the D2 receptor, a change in the FRET fluorescence signal indicates the presence of dopamine. These sensor cells (CNiFERs) were implanted in mice frontal cortex and dopamine release during behavioral conditioning was imaged.

One major advantage of this system is incorporating an endogenous sensor of dopamine (the D2 receptor) as the recognition unit. This means that the kinetics of the sensor, including sensitivity, binding affinity and detection range should be similar to that of endogenous dopamine receptors. The CNiFERs were sensitive and specific with $EC_{50} = 2.5 \pm 0.1$ nM, and a 30 times higher sensitivity for dopamine compared to norepinephrine. However, the temporal resolution of the sensor was on the scale of seconds and the spatial resolution was less than 100 μm due to the size of the implanted HEK cells. Therefore, the spatiotemporal resolution of the sensor was not suitable for resolving release events at a sub-cellular level. Furthermore, the dynamic range was between 1 to 10 nM and the sensor saturated at concentrations close to 100 nM. At individual cells (single sensors), the response to dopamine was detected with 2.9 ± 0.2 s delay after dopamine pulse. The reversibility of the sensor was not instantaneous as the FRET signal would return to baseline in 20 s after a 2.5 s dopamine pulse, which makes detection of fast repetitive or changing dopamine signals more difficult.[77]

The second approach employs engineered fluorescent proteins that bind to dopamine, which causes a direct increase in protein fluorescence. Thus, the protein is the sensor, rather than the whole cell in the case of CNiFERs. Genetically encoded proteins are much smaller than whole cells and therefore ideally suited to detect analytes on the surface or inside of cells. Therefore, there had been a lot of interest in developing a genetically encoded dopamine sensor. The sensor named dLight1 was designed and successfully used to image dopamine dynamics in deep regions of mice brain during behavioural studies (Figure 8).[78] It consists of a genetically modified dopamine receptor that includes a circular permuted GFP module from the genetically encoded calcium indicator GCaMP6 (see structure in Figure 8a). Upon binding of dopamine to its receptor, conformational changes of the receptor are translated to a change in fluorescence intensity of the GFP (Figure 8b). Two variants of the sensor have optimal dissociation constants of $K_d = 330 \pm 30$ nM for dLight1.1 and $K_d = 770 \pm 10$ nM for dLight1.2 (Figure 8c). The sensors are around 70 and 40 times more sensitivity to dopamine than norepinephrine and epinephrine. The maximum concentrations that were detected *in vivo* ranged from 10 μM to 30 μM, indicating proximity to the site of release.[78] This sensor is therefore a useful tool especially for *in vivo* applications. dLight has comparable temporal resolution to cyclic voltammetry. Given the kinetics required for fast detection of dopamine (see Section 3.1) it remains to be seen if this sensor and related ones can detect fast and complex release patterns.

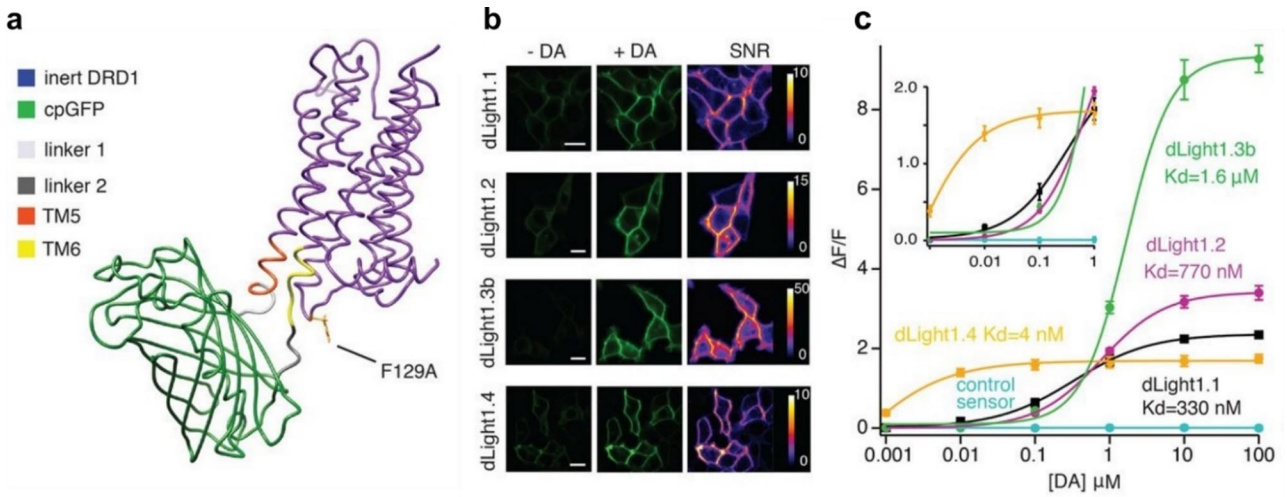

Figure 8. Genetically encoded fluorescent proteins as dopamine sensors. **a**, Structure of the genetically encoded fluorescent probe dLight1 consisting of a DRD1 receptor and cpGFP module. **b**, HEK cells expressing dLight variants. Fluorescence intensity and signal-to-noise ratio (SNR) with and without dopamine are shown. Scale bar = 10 μm. **c**, Calibration curve of various dLight sensors when expressed in HEK cells. Reproduced from reference [78] with permission. Copyright 2018 AAAS, American Association for the Advancement of Science.

Another group also developed a genetically-encoded fluorescent sensor based on the same premise, called GRABDA (G protein-coupled receptor [GPCR]-activation based DA).[79] Two types of sensors were designed, one with a moderate apparent affinity to dopamine (DA1 m, $EC_{50} = 130$ nM) and another with a higher apparent affinity (DA1 h, $EC_{50} = 10$ nM). The EC_{50} of the sensors to norepinephrine was 1.7 μM and 97 nM respectively. The release of dopamine during conditioning behavioural tasks was monitored in mice. A temporal resolution of 100 ms and sub cellular spatial resolution was reported, which is comparable to cyclic voltammetry. When dopamine was applied to cultured cells, the on-rate of the sensor (fluorescence increase) for both DA1 m and DA1 h was fast (60 ± 10 ms for DA1 m and 140 ± 20 ms for DA1 h). However, the off-rate (fluorescence decrease) was slower (2.5 ± 0.3 s for DA1 h and 0.7 ± 0.06 s for DA1 m). In mouse brain slices expressing GRABDA sensors, electrical stimulation of cells produced a fluorescence increase with a rising time constants of 0.1 s for both sensors and decaying time constants of 17 s and 3 s for DA1 h and DA1 m respectively. Although the on-rate of the sensor was very fast, it seems that the slow decaying time of the sensor would preclude detection of fast, individual secretory events.

Genetically encoded sensors require introduction of foreign genetic material encoding the sensor into the host cells (e.g. neurons), usually using viral transduction. Although these genetically encoded sensors offer robust methods with high spatiotemporal resolution for laboratory studies of neural circuits, applying these methods in humans for diagnostic purposes might therefore face challenges because of safety concerns.

5. Fluorescent small molecules

Synthesis of fluorescence false neurotransmitters (FFNs) led to breakthroughs in understanding the kinetics of neurotransmitter uptake, storage and release in monoaminergic cells and neurons. These probes consist of fluorophores with chemical structures similar to neurotransmitters. Gubernator et al.,[80] first designed fluorescent molecules that are substrates of VMAT-2 (vesicular monoamine transporter) and mimic the structure of catecholamines. Therefore, they are differentially uptaken by VMAT-2 from the cytoplasm into vesicles and released through exocytosis when the cells are stimulated. Compared to the classical electrochemical-based methods, these molecular probes can visualise clusters of synaptic vesicles present in dopaminergic axons. FFNs also allowed detection of synaptic vesicle fusion with the plasma membrane upon stimulation of the cells, which is the mechanism by which dopamine is secreted. FFN511 was one of the first of such molecules designed. This molecule binds to VMAT2 in synaptic vesicles with an IC50 of 1 μM.[80] However, FFNs are an indirect method because they mimic neurotransmitters rather than directly detecting endogenous monoamines.

6. Direct imaging of monoamines

Monoamines are weakly fluorescent when directly excited in the UV range, which can be used for direct catecholamine imaging. Using this approach in living organisms is challenging because of the phototoxicity of strong UV light. With this approach, living cells could be imaged with 305 nm laser excitation leading to emission at 350 nm and high spatial resolution (0.22 μm) as well as temporal resolution (50 ms). However, the autofluorescence of the cells at this emission range would confound selective and sensitive monoamine detection.[81] One way to mitigate the UV induced damage to the living cells is to use multi-photon excitation. With two-photon microscopy the UV excitation wavelength is red shifted to longer wavelengths and three-photon microscopy can achieve excitation in the infrared range.[83] Three-photon excitation (3PE) was employed to excite intrinsic UV fluorescence of dopamine, serotonin and tryptophan in the

Table 2. Advantages and limitations of various monoamine sensors.

Monoamine sensors	Advantages	Limitations	Application	References
Fluorescent SWCNTs	Excellent spatial and parallel resolution, minimal bleaching and blinking, Near Infrared fluorescence in the tissue transparency window	Sensors need to be placed in the biological sample.	*In vitro*, Primary cells (platelets), brain slices	Kruss *et al.*,[61] Dinarvand et al.[72] Beyenne et al.[70]
Fluorescent polymer-based particles	Multivalent binding that increases selectivity.	Limited spatial and temporal resolution.	*In vitro*, cell culture, *In vivo*	Cash *et al.*[76]
Fluorescent small molecules	High resolution at subcellular levels.	Indirect imaging, rapid bleaching.	Cell culture, Tissue sections	Gubernator *et al.*[80]
Genetically encoded fluorescent receptors	Suitable temporal resolution, employment of biological monoamines receptors in the detection process.	Less spatial resolution than SWCNT sensors, the need for genetic manipulation.	*In vivo*, Live and freely moving animal models	Patriarchi *et al.*,[78] Sun *et al.*[79]
UV imaging	Label free	Phototoxicity	*In vitro*, Cell culture	Tan *et al.*[81]
PET and SPECT	Clinical application	Low spatial resolution, Expensive (needs a cyclotron on-site)	Clinical diagnosis and patient care	Beliveau et al.[82]

infrared range. Monoamines (serotonin and dopamine) were visualized at granular level (concentrations above 50 mM) the theoretical spatial resolution was <200 nm in the radial directions and ~ 500 nm in the axial direction at 700 nm excitation wavelength.[84] Overall, while UV imaging of monoamines does not require exogenous sensors it will be difficult to translate it to *in vivo* or *in vitro* studies in cells because of the extensive photo-damage by UV light, the weak fluorescence of monoamines and autofluorescence of cellular components in the same emission range.

7. Other non-fluorescent molecular imaging techniques

Radiotracers for PET (positron emission tomography) and SPECT (single photon emission computed tomography) can be used for catecholamine imaging.[85] PET and SPECT are established *in vivo* imaging methods of monoaminergic pathways to understand the pathophysiology of many neurological and psychiatric disorders with broad clinical application, they are non-invasive and highly sensitive. In the case of PET and SPECT a radioactive tracer is injected and gamma rays are detected with 2D cross-sectional scans. A 3D image is then constructed from the 2D scans. However, PET and SPECT have extremely limited spatial resolution.[86] For instance, a high resolution PET imaging system was investigated for constructing a human serotonin brain atlas, which increased the resolution of conventional PET scans from 4.4 mm to an approximate in-plane resolution of 2 mm.[82]

8. Conclusion

Reliable, specific and fast detection of (monoamine) neurotransmitters in biological scenarios has been a major challenge in neuroscience and cell biology to date. The development of such cutting-edge analytical tools for neurotransmitter detection has therefore been a major research focus and the basis for breakthrough discoveries in our understanding of monoamine biology. While electrochemical detection methods have been leading the research on monoamines since the late 1970s, they have been unable to overcome certain limitations with respect to chemical selectivity and spatial resolution. Table 2 outlines the main advantages and disadvantages of the methods discussed in this paper. Recently developed fluorescence-based sensors, both those based on genetically encoded proteins and non-genetically encoded nanomaterials, provide powerful alternatives to older established methods. For example, carbon nanotube-based sensors for dopamine achieved desirable spatial resolution which is required for investigation of monoamine release on the level of individual cellular release sites. Due to their unique properties such as access to the nIR tissue transparency window, such nanosensors are highly promising materials for future studies in neuroscience. Even though translation of these methods into clinical scenarios to facilitate diagnosis and patient care is still a relatively long-term goal the emerging methods summarized in this review article will help to answer long-standing questions in cell biology and neuroscience.

Acknowledgements

We thank the DFG for funding (Kr 4242/4-1). We thank Nils Brose for fruitful discussions and support. Open access funding enabled and organized by Projekt DEAL.

Conflict of Interest

The authors declare no conflict of interest.

Keywords: carbon nanotubes · catecholamines · fluorescence imaging · neuroscience · sensors

[1] E. R. Travis, R. M. Wightman, *Annu. Rev. Biophys. Biomol. Struct.* **1998**, *27*, 77–103.
[2] R. Jahn, D. Fasshauer, *Nature* **2012**, *490*, 201–207.
[3] J. DeFelipe, L. Alonso-Nanclares, J. I. Arellano, *J. Neurocytol.* **2002**, *31*, 299–316.
[4] J. R. Wickens, G. W. Arbuthnott, in *Handb. Chem. Neuroanat.*, Elsevier, **2005**, pp. 199–236.
[5] R. Y. Moore, F. E. Bloom, *Annu. Rev. Neurosci.* **1979**, *2*, 113–168.
[6] K. Racké, A. Reimann, H. Schwörer, H. Kilbinger, *Behav. Brain Res.* **1995**, *73*, 83–87.
[7] I. Papa, D. Saliba, M. Ponzoni, S. Bustamante, P. F. Canete, P. Gonzalez-Figueroa, H. A. McNamara, S. Valvo, M. Grimbaldeston, R. A. Sweet, H. Vohra, I. A. Cockburn, M. Meyer-Hermann, M. L. Dustin, C. Doglioni, C. G. Vinuesa, *Nature* **2017**, *547*, 318–323.
[8] J. Bergquist, A. Tarkowski, R. Ekman, A. Ewing, *Proc. Mont. Acad. Sci.* **1994**, *91*, 12912–12916.
[9] S. J. Cragg, C. Nicholson, J. Kume-Kick, L. Tao, M. E. Rice, *J. Neurophysiol.* **2001**, *85*, 1761–1771.
[10] D. Sulzer, S. J. Cragg, M. E. Rice, *Basal Ganglia* **2016**, *6*, 123–148.
[11] C. Liu, L. Kershberg, J. Wang, S. Schneeberger, P. S. Kaeser, *Cell* **2018**, *172*, 706–718.
[12] J. A. Daniel, S. Galbraith, L. Iacovitti, A. Abdipranoto, B. Vissel, *J. Neurosci.* **2009**, *29*, 14670–14680.
[13] L. Descarries, K. C. Watkins, S. Garcia, O. Bosler, G. Doucet, *J. Comp. Neurol.* **1996**, *375*, 167–186.
[14] M. E. Rice, J. C. Patel, *Philos. Trans. R. Soc. London Ser. B* **2015**, *370*, 20140185.
[15] J. D. Clements, R. A. Lester, G. Tong, C. E. Jahr, G. L. Westbrook, *Science* **1992**, *258*, 1498–1501.
[16] S. J. Cragg, M. E. Rice, *Trends Neurosci.* **2004**, *27*, 270–277.
[17] R. M. Wightman, L. J. May, A. C. Michael, *Anal. Chem.* **1988**, *60*, 769A-793A.
[18] E. S. Bucher, R. M. Wightman, *Annu. Rev. Anal. Chem.* **2015**, *8*, 239–261.
[19] N. Plock, C. Kloft, *Eur. J. Pharm. Sci.* **2005**, *25*, 1–24.
[20] L. M. Borland, G. Shi, H. Yang, A. C. Michael, *J. Neurosci. Methods* **2005**, *146*, 149–158.
[21] F. Gonon, R. Cespuglio, J. L. Ponchon, M. Buda, M. Jouvet, R. N. Adams, J. F. Pujol, *C. R. Acad. Sci. Hebd. Seances Acad. Sci. D.* **1978**, *286*, 1203–1206.
[22] R. M. Wightman, E. Strope, P. M. Plotsky, R. N. Adams, *Nature* **1976**, *262*, 145.
[23] P. T. Kissinger, J. B. Hart, R. N. Adams, *Brain Res.* **1973**, *55*, 209–213.
[24] X. Li, J. Dunevall, A. G. Ewing, *Acc. Chem. Res.* **2016**, *49*, 2347–2354.
[25] M. L. A. V. Heien, M. A. Johnson, R. M. Wightman, *Anal. Chem.* **2004**, *76*, 5697–5704.
[26] J. L. Peters, L. H. Miner, A. C. Michael, S. R. Sesack, *J. Neurosci. Methods* **2004**, *137*, 9–23.
[27] R. G. W. Staal, S. Rayport, D. Sulzer, in *Electrochem. Methods Neurosci.*, CRC Press/Taylor & Francis, **2007**.
[28] I. Hafez, K. Kisler, K. Berberian, G. Dernick, V. Valero, M. G. Yong, H. G. Craighead, M. Lindau, *Proc. Natl. Acad. Sci. USA* **2005**, *102*, 13879–13884.
[29] B. Zhang, M. L. A. V. Heien, M. F. Santillo, L. Mellander, A. G. Ewing, *Anal. Chem.* **2011**, *83*, 571–577.
[30] A. Yakushenko, E. Kätelhön, B. Wolfrum, *Anal. Chem.* **2013**, *85*, 5483–5490.
[31] O. C. Farokhzad, R. Langer, *ACS Nano* **2009**, *3*, 16–20.
[32] D. Brabazon, *Chapter 04103 - Nanostructured Materials*, Elsevier, **2016**.
[33] M. J. O'Connell, S. H. Bachilo, C. B. Huffman, V. C. Moore, M. S. Strano, E. H. Haroz, K. L. Rialon, P. J. Boul, W. H. Noon, C. Kittrell, J. Ma, R. H. Hauge, R. B. Weisman, R. E. Smalley, *Science.* **2002**, *297*, 593–596.
[34] G. Selvaggio, A. Chizhik, R. Nißler, L. Kuhlemann, D. Meyer, L. Vuong, H. Preiß, N. Herrmann, F. A. Mann, Z. Lv, T. A. Oswald, A. Spreinat, L. Erpenbeck, J. Großhans, K. Volker, A. Janshoff, J. Pablo Giraldo, S. Kruss, *Nat. Commun.* **2020**, *11*, 1495.
[35] O. T. Bruns, T. S. Bischof, D. K. Harris, D. Franke, Y. Shi, L. Riedemann, A. Bartelt, F. B. Jaworski, J. A. Carr, C. J. Rowlands, M. W. B. Wilson, O. Chen, H. Wei, G. W. Hwang, D. M. Montana, I. Coropceanu, O. B. Achorn, J. Kloepper, J. Heeren, P. T. C. So, D. Fukumura, K. F. Jensen, R. K. Jain, M. G. Bawendi, *Nat. Biomed. Eng.* **2017**, *1*, 1–11.
[36] S. Kruss, A. J. Hilmer, J. Zhang, N. F. Reuel, B. Mu, M. S. Strano, *Adv. Drug Delivery Rev.* **2013**, *65*, 1933–1950.
[37] E. Polo, S. Kruss, *Anal. Bioanal. Chem.* **2016**, *408*, 2727–2741.
[38] Q. Mu, H. Xu, Y. Li, S. Ma, X. Zhong, *Analyst* **2014**, *139*, 93–98.
[39] J. Zhao, L. Zhao, C. Lan, S. Zhao, *Sensors Actuators B Chem.* **2016**, *223*, 246–251.
[40] X. Zhang, X. Chen, S. Kai, H.-Y. Wang, J. Yang, F.-G. Wu, Z. Chen, *Anal. Chem.* **2015**, *87*, 3360–3365.
[41] K. Fuxe, D. O. Borroto-Escuela, W. Romero-Fernandez, Z. Diaz-Cabiale, A. Rivera, L. Ferraro, S. Tanganelli, A. O. Tarakanov, P. Garriga, J. A. Narváez, F. Ciruela, M. Guescini, L. F. Agnati, *Front. Physiol.* **2012**, *3*, 136.
[42] E. V. Mosharov, A. Borgkvist, D. Sulzer, *Mov. Disord.* **2015**, *30*, 45–53.
[43] D. Meyer, A. Hagemann, S. Kruss, *ACS Nano* **2017**, *11*, 4017–4027.
[44] C. Cha, S. R. Shin, N. Annabi, M. R. Dokmeci, A. Khademhosseini, *ACS Nano* **2013**, *7*, 2891–2897.
[45] G. Hong, S. Diao, A. L. Antaris, H. Dai, *Chem. Rev.* **2015**, *115*, 10816–10906.
[46] M. S. Dresselhaus, G. Dresselhaus, P. C. Eklund, A. M. Rao, in (Ed.: W. Andreoni), Springer Netherlands, Dordrecht, **2000**, pp. 331–379.
[47] V. K. K. Upadhyayula, V. Gadhamshetty, *Biotechnol. Adv.* **2010**, *28*, 802–816.
[48] G. Hong, S. Diao, J. Chang, A. L. Antaris, C. Chen, B. Zhang, S. Zhao, D. N. Atochin, P. L. Huang, K. I. Andreasson, *Nat. Photonics* **2014**, *8*, 723–730.
[49] A. Spreinat, G. Selvaggio, L. Erpenbeck, S. Kruss, *J. Biophotonics* **2020**, *13*, 1–8.
[50] R. Nißler, F. A. Mann, H. Preiß, G. Selvaggio, N. Herrmann, S. Kruss, *Nanoscale* **2019**, *11*, 11159–11166.
[51] M. Zheng, A. Jagota, E. D. Semke, B. A. Diner, R. S. McLean, S. R. Lustig, R. E. Richardson, N. G. Tassi, *Nat. Mater.* **2003**, *2*, 338–342.
[52] F. A. Mann, J. Horlebein, N. F. Meyer, D. Meyer, F. Thomas, S. Kruss, *Chem. Eur. J.* **2018**, *24*, 12241–12245.
[53] G. Bisker, J. Dong, H. D. Park, N. M. Iverson, J. Ahn, J. T. Nelson, M. P. Landry, S. Kruss, M. S. Strano, *Nat. Commun.* **2016**, *7*, 1–14.
[54] E. Polo, T. T. Nitka, E. Neubert, L. Erpenbeck, L. Vuković, S. Kruss, *ACS Appl. Mater. Interfaces* **2018**, *10*, 17693–17703.
[55] J. Budhathoki-Uprety, J. D. Harvey, E. Isaac, R. M. Williams, T. V. Galassi, R. E. Langenbacher, D. A. Heller, *J. Mater. Chem. B* **2017**, *5*, 6637–6644.
[56] J. D. Harvey, H. A. Baker, M. V. Ortiz, A. Kentsis, D. A. Heller, *ACS Sens.* **2019**, *4*, 1236–1244.
[57] A. Hendler-Neumark, G. Bisker, *Sensors* **2019**, *19*, 5403.
[58] F. A. Mann, Z. Lv, J. Grosshans, F. Opazo, S. Kruss, *Angew. Chem. Int. Ed.* **2019**, *58*, 11469–11473.
[59] J. P. Giraldo, H. Wu, G. M. Newkirk, S. Kruss, *Nat. Nanotechnol.* **2019**, *14*, 541–553.
[60] H. Wu, R. Nißler, V. Morris, N. Herrmann, P. Hu, S. J. Jeon, S. Kruss, J. P. Giraldo, *Nano Lett.* **2020**, *20*, 2432–2442.
[61] S. Kruss, M. P. Landry, E. Vander Ende, B. M. A. Lima, N. F. Reuel, J. Zhang, J. Nelson, B. Mu, A. Hilmer, M. Strano, *J. Am. Chem. Soc.* **2014**, *136*, 713–724.
[62] F. A. Mann, N. Herrmann, D. Meyer, S. Kruss, *Sensors* **2017**, *17*, 1521.
[63] E. Polo, S. Kruss, *J. Phys. Chem. C* **2016**, *120*, 3061–3070.
[64] R. Nißler, F. A. Mann, P. Chaturvedi, J. Horlebein, D. Meyer, L. Vuković, S. Kruss, *J. Phys. Chem. C* **2019**, *123*, 4837–4847.
[65] S. Kruss, D. P. Salem, L. Vuković, B. Lima, E. Vander Ende, E. S. Boyden, M. S. Strano, *Proc. Mont. Acad. Sci.* **2017**, *114*, 1789–1794.
[66] G. Bisker, J. Ahn, S. Kruss, Z. W. Ulissi, D. P. Salem, M. S. Strano, *J. Phys. Chem. C* **2015**, *119*, 13876–13886.
[67] A. J. Lee, X. Wang, L. J. Carlson, J. A. Smyder, B. Loesch, X. Tu, M. Zheng, T. D. Krauss, A. J. Lee, X. Tu, M. Zheng, T. D. Krauss, *Nano Lett.* **2011**, *11*, 1636–1640.

[68] A. J. Gillen, J. Kupis-Rozmysł Owicz, C. Gigli, N. Schuergers, A. A. Boghossian, *J. Phys. Chem. Lett.* **2018**, *9*, 4336–4343.
[69] A. G. Godin, J. A. Varela, Z. Gao, N. Danné, J. P. Dupuis, B. Lounis, L. Groc, L. Cognet, *Nat. Nanotechnol.* **2017**, *12*, 238–243.
[70] A. G. Beyene, K. Delevich, J. T. Del Bonis-O'Donnell, D. J. Piekarski, W. C. Lin, A. Wren Thomas, S. J. Yang, P. Kosillo, D. Yang, G. S. Prounis, L. Wilbrecht, M. P. Landry, *Sci. Adv.* **2019**, *5*, eaaw3108.
[71] D. Meyer, S. Telele, A. Zelená, A. J. Gillen, A. Antonucci, E. Neubert, R. Nißler, F. A. Mann, L. Erpenbeck, A. A. Boghossian, S. Köster, S. Kruss, *Nanoscale* **2020**, *12*, 9104–9115.
[72] M. Dinarvand, E. Neubert, D. Meyer, G. Selvaggio, F. A. Mann, L. Erpenbeck, S. Kruss, *Nano Lett.* **2019**, *19*, 6604–6611.
[73] K. S. Hettie, T. E. Glass, *ACS Chem. Neurosci.* **2016**, *7*, 21–25.
[74] H. N. Kim, Z. Guo, W. Zhu, J. Yoon, H. Tian, *Chem. Soc. Rev.* **2011**, *40*, 79–93.
[75] C.-G. Qian, S. Zhu, P.-J. Feng, Y.-L. Chen, J.-C. Yu, X. Tang, Y. Liu, Q.-D. Shen, *ACS Appl. Mater. Interfaces* **2015**, *7*, 18581–18589.
[76] K. J. Cash, H. A. Clark, *Sensors* **2012**, *12*, 11922–11932.
[77] A. Muller, V. Joseph, P. A. Slesinger, D. Kleinfeld, *Nat. Methods* **2014**, *11*, 1245.
[78] T. Patriarchi, J. R. Cho, K. Merten, M. W. Howe, A. Marley, W.-H. Xiong, R. W. Folk, G. J. Broussard, R. Liang, M. J. Jang, H. Zhong, D. Dombeck, M. von Zastrow, A. Nimmerjahn, V. Gradinaru, J. T. Williams, L. Tian, *Science* **2018**, *360*, eaat4422.
[79] F. Sun, J. Zeng, M. Jing, J. Zhou, J. Feng, S. F. Owen, Y. Luo, F. Li, H. Wang, T. Yamaguchi, Z. Yong, Y. Gao, W. Peng, L. Wang, S. Zhang, J. Du, D. Lin, M. Xu, A. C. Kreitzer, G. Cui, Y. Li, *Cell* **2018**, *174*, 481–496.e19.
[80] N. G. Gubernator, H. Zhang, R. G. W. Staal, E. V. Mosharov, D. B. Pereira, M. Yue, V. Balsanek, P. A. Vadola, B. Mukherjee, R. H. Edwards, D. Sulzer, D. Sames, *Science* **2009**, *324*, 1441–1444.
[81] W. Tan, V. Parpura, P. G. Haydon, E. S. Yeung, *Anal. Chem.* **1995**, *67*, 2575–2579.
[82] V. Beliveau, M. Ganz, L. Feng, B. Ozenne, L. Højgaard, P. M. Fisher, C. Svarer, D. N. Greve, G. M. Knudsen, *J. Neurosci.* **2017**, *37*, 120–128.
[83] B. K. Maity, S. Maiti, *Neuronal Signal.* **2018**, *2*, DOI 10.1042/ns20180132.
[84] S. Maiti, J. B. Shear, R. M. Williams, W. R. Zipfel, W. W. Webb, *Science* **1997**, *275*, 530–532.
[85] J. C. Soares, R. B. Innis, *Biol. Psychiatry* **1999**, *46*, 600–615.
[86] V. Kaasinen, J. O. Rinne, *Neurosci. Biobehav. Rev.* **2002**, *26*, 785–793.

Manuscript received: March 27, 2020
Revised manuscript received: June 5, 2020
Accepted manuscript online: June 11, 2020